ACS APPLIED MATERIALS & INTERFACES

Research Article

www.acsami.org

Tunable, Functional Carbon Spheres Derived from Rapid Synthesis of Resorcinol-Formaldehyde Resins

Vilas G. Pol,*[,†,‡] Lok Kumar Shrestha,[‡] and Katsuhiko Ariga[‡]

[†]School of Chemical Engineering, Purdue University, West Lafayette, Indiana 47907, United States

[‡]World Premier International Center for Materials Nanoarchitechtonics (WPI-MANA), National Institute for Materials Science (NIMS), 1-1 Namiki, Tsukuba 305-0044, Japan

ABSTRACT: In this article, the rapid synthesis of colloidal, spherical polymer resins via enhanced copolymerization and polycondensation of resorcinol with formaldehyde is presented. The ultrasound-mediated technique assembles perfectly spherical resins in less than 5 min due to generated active species and free radicals produced in an aqueous ammonia−ethanol−water solvent. In this report, numerous controlled experiments account for and support the important role of high intensity ultrasounds in the rapid cluster formation, condensation, and gelation process of resorcinol with formaldehyde in the presence of ammonia catalyst. After a controlled heat treatment process, amorphous carbon spheres are obtained from these spherical polymer resins. The effect of temperature (up to 1100 °C) on the structural evolution of these carbon spheres is meticulously studied which is lacking in the previous literature. The resorcinol−formaldehyde resins carbonized at 600 and 900 °C demonstrate BET surface areas of 592.4 m^2/g and 952.5 m^2/g with specific capacitances of 17.5, and 33.5 F/g (scan rate of 5 mV/s), respectively.

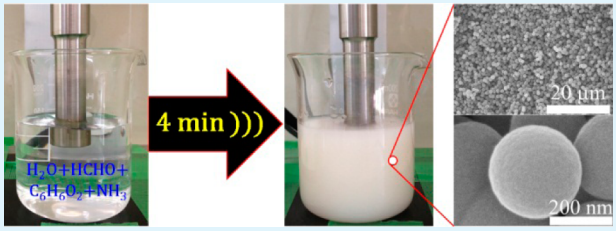

KEYWORDS: *colloids, energy storage, polymers, copolymerization, ultrasonic, carbon spheres*

1. INTRODUCTION

Colloidal spherical particles are an attractive research area in a multitude of fields due to their large amount of multidisciplinary plausible applications including energy storage devices,[1,2] drug delivery,[3,4] photonic crystals,[5,6] sensors,[7−9] and catalytic supports.[10,11] Initial reports about preparing organic aerogels and xerogels by hydrolysis and condensation reactions in aqueous solvents[12,13] ignited the research interests across many disciplines of the scientific community. Carbonaceous materials derived from resorcinol (R)-formaldehyde (F) gels are promising candidates for numerous applications due to their controllable pore structures, spherical nature, high porosities, excellent thermal properties, and significant electrical conductivities.[14−16]

In 1968, Stöber et al. reported a process to synthesize monodispersed inorganic silica particles[17] via the hydrolysis and condensation of tetraethyl orthosilicate using an aqueous ammonia catalyst in an alcohol−water solvent. Ultimately, it has become scientifically interesting to extend the Stöber process to carbonaceous spheres. Using sodium carbonate as a catalyst, spherical polymeric resins have been derived from the reaction of R and F in an aqueous medium at 85 °C in 24 h.[18] Similarly, the condensation of R and F requires longer time in the presence of sodium carbonate[19,20] and several hours in the presence of magnesium acetate catalyst[21] or basic amino acid-assisted[22] synthesis. Liu et al. demonstrated that the Stöber method can be used to synthesize monodispersed RF resin polymers using an ammonia catalyst in a water/ethanol solvent at 100 °C for 24 h in Teflon lined autoclave.[23] In 2011, advances in the tailoring of RF organic gel review was focused on various reaction conditions such as the catalyst type (except ammonia), solvent concentration, precursor concentrations, reaction time, drying method, and temperature of curing.[14] Finally, rapid synthesis has been achieved in the creation of nitrogen-doped nonspherical porous carbon in 5 min by copolymerization of R and F with basic amino acid lysine[24] catalyst. Zhu et al. reported sol−gel process derived porous carbon materials with KOH activation yielding 522 to 2760 m^2/g BET surface area and 294 F/g capacitance.[25] Horikawa et al. synthesized aerogel RF spherical particles with 10 to 500 μm diameters in a basic aqueous solution followed by carbon dioxide supercritical drying possessing.[26] Recently, many other researchers reported on the synthesis of R-F derived polymers followed by carbonization achieving porous carbon materials.[27−31] However, our RF resins are spherical in nature and can be synthesized in an aqueous solution in less than 5 min. In addition, the effect of thermal treatment (up to 1100 °C) on the textural changes of the gel is also included in this report, which is also missing from the previous literature.

2. MATERIALS AND METHODS

2.1. Rapid Synthesis of Spherical RF-Resins. Spherical RF-resins were synthesized under ultrasonic irradiation (Ultrasonic Generator, model GSCVP 150) using solid resorcinol $(C_6H_4OH)_2$

Received: April 16, 2014
Accepted: June 10, 2014
Published: June 10, 2014

and formaldehyde solution (HCHO, 37 wt % in aqueous solution stabilized by 10% methanol) as chemical precursors. The solvent solutions were prepared in 250 mL beakers by homogenizing 100 mL of deionized water (H_2O), 40 mL of absolute ethanol (EtOH) and 0.5 mL of ammonia aqueous solution (NH_4OH, 25 wt %) in 10 s of sonochemical tip irradiation under 80% power. In the aforementioned solution, 1 g of resorcinol was dissolved followed quickly by 1.4 mL of formaldehyde. This mixture was then sonochemically irradiated for 2 to 5 min to obtain milky white spherical resins composed of resorcinol and formaldehyde. Since the sonochemical irradiation of solvents increases the reaction temperature, an ice bath was implemented to maintain a reaction temperature between 15 and 25 °C. The solid product was then recovered and water/ethanol washed using a centrifuge to remove excess ammonia. Finally, the pure resins were vacuum-dried at 50 °C for 4 h.

2.2. Preparation of Carbon Spheres (CS). The dried, brownish, spherical RF resins were transferred into a crucible placed in a furnace chamber, evacuated then purged with N_2 atmosphere. The resins were subsequently heated with a heating rate of 1−2 °C/min to 600 °C (ADVANTEC Type: FUA112DB). After holding the furnace temperature at 600 °C for 3 h, the furnace was then cooled to room temperature with a 10 °C/min cooling rate. The postcarbonized, monolithic carbon spheres retained about 54 wt % of the original resin mass. In a similar fashion, RF resins were heat treated to 900 °C termed as (CS900) and 1100 °C (CS1100) in the same inert atmospheric conditions. For each sample, the holding time was set for 3 h and the cooling was carried out at a rate of 10 °C/min. After cooling down, the obtained materials were used for further characterization and electrochemical testing.

2.3. Characterization. Surface functional groups of the as-prepared carbon spheres were determined by recording FTIR spectra on the Thermo Electron Corporation, Nicolet 4700 at 25 °C. The percent transmission of the samples were recorded over 400−4000 cm^{-1}. The change in the graphitic nature in the carbon spheres were recorded by Rigaku X-ray diffractometer, RINT, operated at 40 kV and 40 mA with Cu−Kα radiation at 25 °C. The diffractograms were recorded in the 2θ range from 10 to 50° with a 2θ step size of 0.02 and a scanning speed of 2 deg/min. Raman scattering spectra were recorded with a Jobin-Yvon T64000. The samples for Raman scattering were prepared on clean a glass substrate and the samples were excited using green laser (514.5 nm and 0.05 mW power). Thermogravimetric measurements (TG) were conducted using a Seiko Instruments thermogravimetry/differential thermal analyzer TG-DTA 6200. The TG was performed with a temperature sweep from room temperature to 1000 °C at a heating rate of 2 °C/min under an argon flow of 100 mL/min in an open alumina pan. Scanning electron microscopy (SEM) images were recorded using S-4800, Hitachi Co. Ltd. operated at 10 kV.

Transmission electron microscopy (TEM) images, high resolution-TEM (HR-TEM) images, and selected area electron diffraction (SAED) patterns were taken from the smallest components of carbons using a JEOL Model JEM-2100F transmission electron microscope operated at 200 kV. TEM samples were prepared by drop casting a dilute suspension of carbon spheres in alcohols on a carbon-coated copper grid. Prior to obtaining TEM images, the sample was dried in reduced pressure for 24 h. N_2 adsorption−desorption isotherms were recorded using an automatic adsorption instrument (Quantachrome Instrument, Autosorb-1 U.S.A.) in order to determine the surface areas of the samples. For each measurement about 80 mg of activated carbon was taken and degassed for 24 h at 100 °C prior to the measurement. The adsorption−desorption isotherms were recorded at a liquid nitrogen temperature of 77.35 K. The specific surface area was calculated using the Brunauer−Emmett−Teller (BET) method.

2.4. Cyclic Voltammetry. In addition to physical characterization, electrochemical characterization of the separate heat-treated carbon sphere samples was performed. This was done by recording cyclic voltammograms (CVs) at different scan rates (5, 10, 20, 50, 80, and 100 mV/s). Measurements were then performed using an Electrochemical Analyzer, Model 850 BZ, ALS/CH instruments in the potential range of (−0.2 to 1.2 V vs Ag/AgCl) using 1 M H_2SO_4 aqueous solution as an electrolyte.

3. RESULTS AND DISCUSSION

The mixture of resorcinol and formaldehyde in a water−alcohol solvent prepared a transparent solution under 10 s of ultrasonic irradiation (Scheme 1, left panel). After adding the ammonia

Scheme 1. Schematic of the Formation of Spherical RF Resins under Rapid (< 5 min) Sonochemical Irradiation

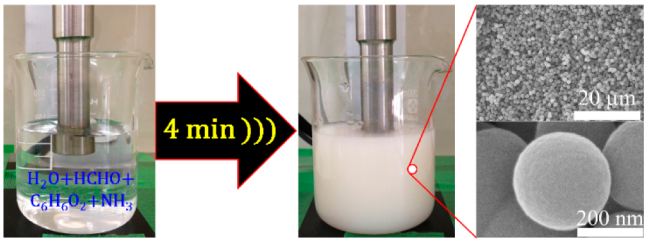

catalyst and ultrasonically irradiating the solution continuously for 3 min, the resulting solution displayed a pale brown color. This solution then turned to milky white precipitate after total 4 min of ultrasonic irradiation (Scheme 1 right panel).

The rapid synthesis of our RF resins can be explained by sonochemical effects on current experiments. Ultrasonic irradiation drives chemical reactions under extreme pressures and temperatures. These conditions are caused by the continuous nucleation, bubble growth, and impulsive collapse of cavitating bubbles in the solvents present in sonochemical synthesis processes.[32] During the implosive bubble collapse, hot spots are generated that excite water molecules into vibrational, rotational, and electronic states via inelastic collisions.[33] This provides sufficient energy to dissociate water vapor into H• and OH• radicals.[34] Such ultrasound assisted chemical reactions are known for increasing reaction rates, altering the reaction path and allowing the reaction to occur in milder reaction conditions (e.g., lowering the reaction temperature).[35] In addition, these methods can be used to initiate polymerization reactions and shorter gelation (cross-linking) time.

Interestingly, RF sonogels obtained previously by employing ultrasonic irradiation (50−130 min) in a basic sodium carbonate catalyst followed by carbonization at 850 °C was not spherical in shape.[36] In contrast, our RF materials are spherical in nature. This can be explained by the important role of ammonia catalyst in the copolymerization of resorcinol. This process is initiated by aminomethylates containing two active hydrogens and an iminium ion[37] generated from an amine in the presence of formaldehyde. Moreover, the organic sol−gel process of RF resins formation is similar to the inorganic silicate sol−gel process attaining similar 3D networks with four coordination sites and a tetrahedral coordination geometry.[38] However, the rate of our RF formation reaction is dramatically enhanced with ultrasonic irradiation as a result of the generated free radicals and active species.[35] These induce the formation of hydroxymethyl-substituted species[37] on the surfaces which is followed by electrostatic interaction with the ammonia molecules. This process eventually leads to rapid cross-linking, cluster formation, condensation, and gelation.

The scanning electron micrograph (Figure 1a) exhibits that RF spheres have diameters of approximately 900 nm and possess smooth surfaces. In addition, notice that the slow-heating carbonization process to 600 °C (Figure 1b) does not

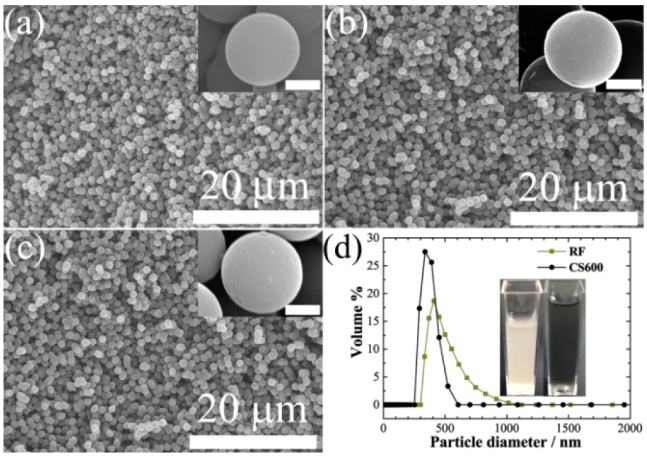

Figure 1. (a) SEM image of sonochemically fabricated as-prepared spherical RF-resins, (b) SEM image of material a heat treated to 600 °C/3 h in an inert atmosphere (CS600), (c) SEM of RF-resins carbonized at 900 °C (CS900). Insets of panel a to c shows high resolution SEM images. Scale bars represent 500 nm, and (d) DLS plots of separate batch of spherical RF-resins (485 nm) and CS600 [inset: photograph demonstrating the dispersion of the RF- resins (white) and carbon spheres (black) in ethanol with mild bath sonication].

change the spherical morphology or surface smoothness of the material. Similarly, the RF resins that were further heated to 900 °C also completely retain their spherical shape (Figure 1c). The continued sonication up to 1 h does not show any theatrical effect on the shape or size of the RF resins.

The particle sizes of the RF resins were shown to decrease when doubling the NH_4OH concentration from 0.25 to 0.5 mL in the presence of the same ethanol/water volume to RF ratio at 15−20 °C. In this experiment, though the ammonia concentration was higher the reaction temperature was lower which led to fabrication of smaller spherical size RF-resins with mostly having average particle diameters of around 415 nm. Around 20% shrinkage in the overall particle size is observed in the DLS (Figure 1d) and SEM after the slow heat rate carbonization process to 600 °C for 3 h. Such uniform RF (415 nm) and carbon spheres (~320 nm) can be suspended in ethanol for long periods of time after undergoing mild bath sonication. The SEM images of submicrometer size uniform RF and carbon spheres particles are shown in Figure 2.

During the rapid sonochemical synthesis of RF-spheres, a small fraction of the particles merged due to the enhanced rate of polymerization and emulsification process. This can be seen in the SEM image in Figure 3a and b.

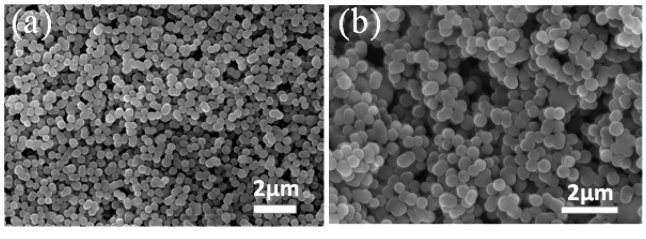

Figure 2. (a) SEM of spherical RF-resins (415 nm) prepared at higher concentration of ammonia, (b) RF resins further heat-treated to 600 °C for 3 h.

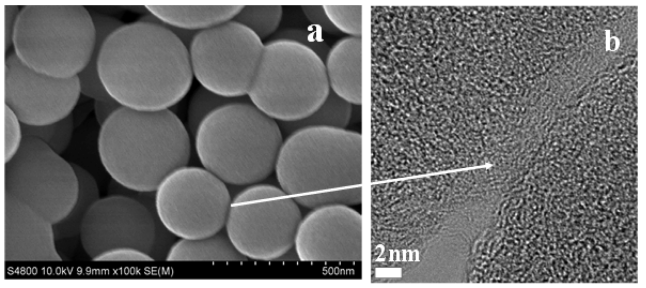

Figure 3. (a) SEM and (b) HR-TEM of merged resorcinol−formaldehyde spheres due to accelerated polymerization and emulsification process.

Holding all other reaction conditions constant, a control RF emulsion and polymerization reaction was carried out for 24 h with continuous stirring and no sonication. This reaction yielded micrometer size and mostly aggregated particles (Figure 4), alluding to the importance of ultrasound in maintaining the spherical shape of the particles.

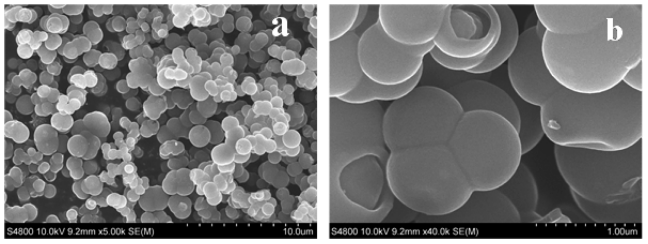

Figure 4. (a) SEM and (b) HR-SEM of a control experiment: RF emulsion and polymerization reaction carried out for 24 h with continuous stirring and no sonication; all other reaction conditions held constant.

Since none of the previous RF resins related publications demonstrate a methodical structural evolution of carbonaceous material as a function of temperature; efforts were made to understand this process using HR-TEM, XRD, Raman spectroscopy and FT-IR spectroscopy.

The TEM and respective HR-TEM are shown in Figure 5. The TEM of single particles were taken at lower resolution to observe the overall surface roughness of the RF resins and carbonized resins. Though the surface of RF resins remained smooth after carbonizing at 600 °C, the surfaces becomes coarser for the samples heated at higher temperatures (CS-900 and CS-1100). In the carbonization process, chemical bonds thermally break in the presence of an inert nitrogen or argon atmosphere.

During the high temperature carbonization of RF resin, loss of hydrogen and oxygen atoms takes place. This further promotes the evolution of dimensional nanolayers improving the structural network within carbon.[39] This structural evolution and ordering of carbon layers is clearly evidenced in the TEM of heated spheres. The selected area electron diffraction pattern also confirmed the appearance of (002) plane in the 900 °C sample and the 1100 °C sample. In addition, the (002) and (101) planes are also present in 1100 °C sample (Figure 6). In this manner, the carbonization process converts electrically insulating polymeric RF resins into a conducting carbon matrix thus yielding materials with potential applications as catalyst supports and electrode

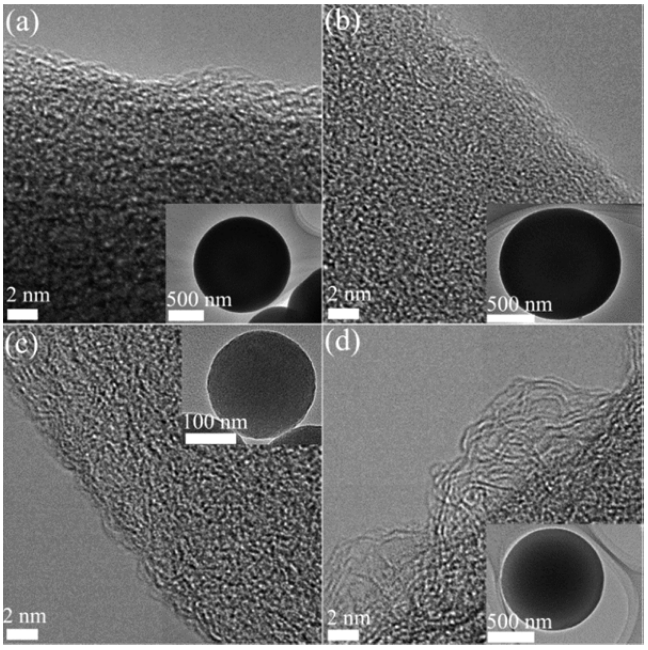

Figure 5. (a) HR-TEM image of RF resin (inset shows low resolution electron micrograph of a single RF resin), (b) HR-TEM image of CS600 (inset shows low resolution electron micrograph of a single CS600), (c) corresponding electron micrographs for CS900, and (d) for CS1100.

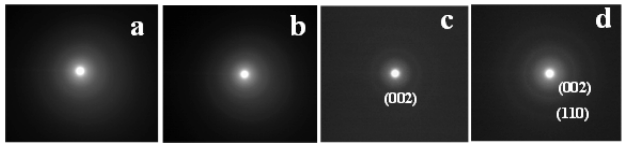

Figure 6. Electron diffraction patterns of (a) RF resins, (b) RF resins heat treated to 600 °C, (c) RF resins heat treated to 900 °C, and (d) RF resins heat treated to 1100 °C in an inert atmosphere.

materials. The electron energy loss spectroscopy (EELS) also corroborated to the HR-TEM and ED observation.

To understand whether it is the surface effect or the bulk structural evolution within the carbon spheres, we have methodically carried out Raman spectroscopy and powder X-ray diffractions on CS600, CS900, and CS1100 samples. The broad Raman bands (Figure 7) appeared at ~1340 cm^{-1} (denoted as D-band) belong to A_{1g} symmetry, which generally refers to the disorder nature of carbon and its structural defects.[2] The narrow G-band appearing at ~1585 cm^{-1} indicates sp^2-bonded carbon atoms in 2-D hexagonal lattice having E_{2g} symmetry.[40] The comparative intensity ratio of the D- and G-bands (I(D)/I(G)) is 1.1. At the low carbonization temperature of the spherical RF resins, the local order of formed carbonaceous layers is poor and might have some dangling bonds since 600 °C is not a high enough temperature to progress the graphitic order without any metal catalyst (e.g., Fe, Ni, Co, etc.). These spherical RF resins heated to higher temperatures (900 and 1100 °C) however, display a decrease in the full width at half-maximum (fwhm) values of D- and G-Raman bands as the formation of a planar graphite structure[41] is observed (Figure 7).

The XRD pattern of CS600 shows weak but broad X-ray reflections at around 25 and 43° 2θ. These broad XRD peaks, which are assigned to (002) and (101) planes of carbon,

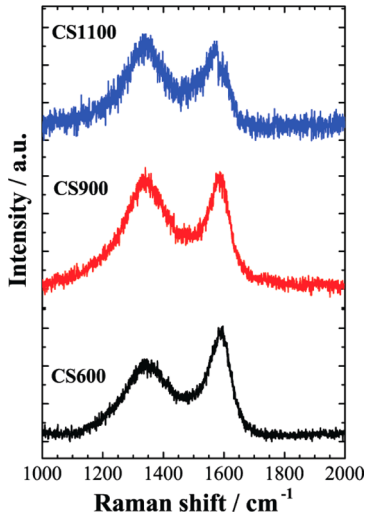

Figure 7. Raman spectra of RF resins heat treated to 600 °C (CS600), RF resins heat treated to 900 °C (CS900), and RF resins heat treated to 1100 °C (CS1100) in an inert atmosphere.

become more prominent for the CS900 and CS1100 samples suggesting a turbostratic structure.[42] Interestingly, the XRD pattern of RF-resins also showed big hump at around 20° 2θ (Figure 8).

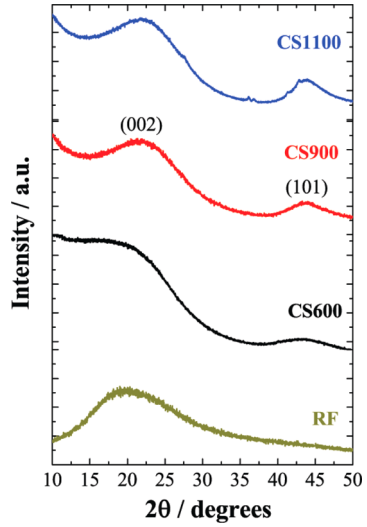

Figure 8. XRD patterns of RF resin, CS600, CS900, and CS1100.

In the FT-IR spectra of spherical RF resins, the broad peak centered at 3200 cm^{-1} is characteristic of the presence of stretching vibration of hydroxyl −OH group, which is related to adsorbed water. The peak at 1455 cm^{-1} corresponds to the $-CH_2$ groups and the peak at 1614 cm^{-1} signifies an aromatic group such as a carbonyl. In between 1000 and 1300 cm^{-1}, numerous peaks are observed corresponding to C−O−C groups and alkyl-phenyl ether.[43] In RF resins, additional functional groups near 700 cm^{-1} are associated with the out-of-plane deformation vibration of C−H as well as out-of plane bending of −OH groups.[44] Some of these stretching vibrations (1614 cm^{-1}, 1455 cm^{-1}, 880 cm^{-1}, etc.) are still available in the CS600 sample, indicating that this temperature is not sufficient to remove all these groups. However, at 900 °C, most of these vibrational groups were removed as shown by the FT-IR

spectrum of CS900. This indicates that this is the required temperature in order to remove all these groups (Figure 9).

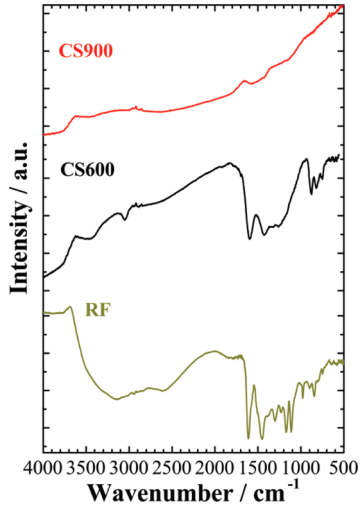

Figure 9. FT-IR spectra of RF resin, CS600, CS600, and CS900 recorded at 25 °C.

The thermogravimetric analysis (TGA) curve of the sonochemically derived spherical RF resins in an inert argon atmosphere is shown in Figure 10a. The intricate thermal

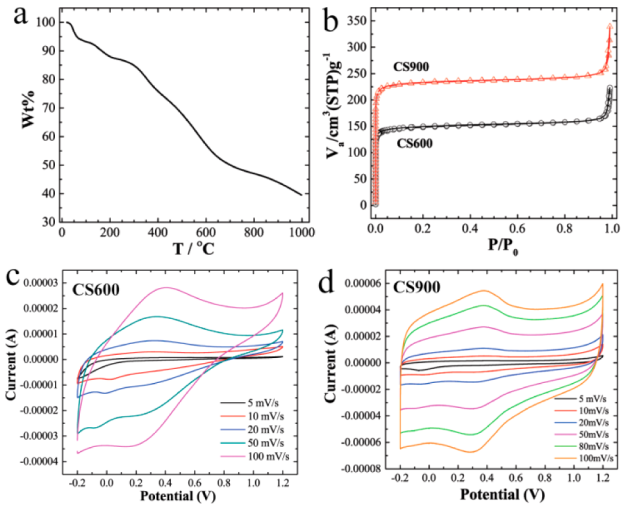

Figure 10. (a) TGA of RF resins in an Ar-atmosphere, (b) nitrogen adsorption/desorption isotherms of the carbon spheres obtained after heat treatment of RF resins at 600 and 900 °C, respectively, (c) CV curves of CS600, and (d) CV curves of CS900 in a 1 M H_2SO_4 aqueous electrolyte solution within a potential range from −0.2 to 1.2 V versus Ag/AgCl reference electrode.

decomposition process is evidenced by a multistep weight loss in the entire temperature range. This continuous, slow weight loss can be ascribed to the transformation of a thermally unstable RF polymer (containing C, H, and O) to a stable carbonaceous material. During the carbonization process in an inert atmosphere, the remaining solvent or H_2O is released via condensation of −OH groups (at <200 °C), then the hydrogen, oxygen or hydrocarbons such as CO_2 and CH_4 (at 380 °C). Finally, aromatization follows at temperatures around 600 °C. These observations are directly reflected on the differential thermal analysis curve. After heat treatment, the remaining sample masses of the 600 and 900 °C samples were estimated to be around 57 and 44 wt % carbon, respectively. These results were similar (5% deviation) to the obtained carbonization yield carried out employing analogous heating and cooling rates in an inert atmosphere. Analogous weight losses were reported for the monodisperse polypyrrole nanospheres (<100 nm) synthesized using ultrasonic polymerization of pyrrole monomers[45] in the presence of a ferric chloride catalyst after carbonizing in a nitrogen atmosphere.

RF resins carbonized at 600 and 900 °C produced microporous carbons. As shown in Figure 10b, N_2 adsorption/desorption isotherms of CS600 and CS900 samples show a typical Type I isotherm with two sharp uptakes at low (p/p_0< 0.10) and high (p/p_0 < 0.9) relative pressures, respectively. This not only indicates that they are microporous materials but also shows that there is some possibility of small macropores existing within the structure. The BET surface area measurement for carbon spheres obtained via the carbonization of 415 nm resins at 600 °C is ca. 592 m^2/g. This value increases with carbonization at higher temperature (900 °C) yielding a BET surface area of 952.5 m^2/g.

Furthermore, we studied the electrochemical performance of the CS600 and CS900 samples to test their potentiality as supercapacitor electrodes. Parts c and d of Figure 10 present cyclic voltammograms (CVs) of CS600 and CS900 at different scan rates (5, 10, 20, 50, 80, and 100 mV/s). These measurements are made in a 1 M H_2SO_4 aqueous electrolyte solution within a potential range of −0.2 to 1.2 V versus a Ag/AgCl reference electrode. All CV curves show sudden current responses on the voltage reversal at each end potential.[46] Note that these shapes are not perfectly rectangular because of the equivalent series electrode resistance.[47] In constrast, for an ideal supercapacitor, rectangular shape CV curves should be seen. However, in a real system, the electrolyte ion diffusion may be prevented by the migration force and the polarized resistance, which makes the CV curve different from the ideal rectangle. Notice in Figure 10c−d that the CV curves of CS600 show higher deviation from the ideal shape whereas the curves of CS900 show rectangle-like shape. This demonstrates faster electrolyte ion diffusion and higher performance capacitor device from the CS900 material. Conversely, the poor electrochemical performance of CS600 is expected due to incomplete carbonization. The specific capacitance of CS600 and CS900 is ca. 17.5, and 33.5 F/g at scan rate 5 mV/s. Mesoporous[48] carbon spheres fabricated from template based structured mesoporous silica via chemical vapor deposition of ethylene produced a high surface area of 666.8 m^2/g and the specific capacity of 59 F/g. Hydrothermally prepared monodispersed carbon spheres from glucose[49] were activated with molten KOH treatment. As-prepared spherical carbon produced 1670 m^2/g BET surface area and yielded high specific[49] capacitance of 253 F/g.

Recently reported sulfur[50] doped carbons and organic xerogels derived carbons[51] are also promising materials for energy storage devices. Our sonochemically fabricated tunable spherical carbon particles also may have a great promise as electrode materials for lithium and sodium ion batteries. These applications are currently under investigation.

4. CONCLUSIONS

In this study, the accelerated copolymerization and polycondensation of resorcinol with formaldehyde is observed in an ethanol−water solvent while maintaining reaction temperature

between 15 and 25 °C. This reaction was carried out in the presence of aqueous ammonia and sonochemically generated H• and OH• radicals. This novel, promising approach allows for the synthesis of colloidal RF particles in a short time (<5 min). These particles can then be converted to submicrometer sized purely carbonaceous particles. Furthermore, the porous carbon particles are potential candidates as materials for Li-ion storage, catalyst supports, and adsorbents.

AUTHOR INFORMATION

Corresponding Author

*Email: vpol@purdue.edu.

Notes

The authors declare no competing financial interest.

ACKNOWLEDGMENTS

V.P. is thankful to start-up funds provided by the Purdue School of Chemical Engineering and College of Engineering to support part of this work.

REFERENCES

(1) Jin, Y. Z.; Kim, Y. J.; Gao, C.; Zhu, Y. Q.; Huczko, A.; Endo, M.; Kroto, H. W. High Temperature Annealing Effects on Carbon Spheres and their Applications as Anode Materials in Li-ion Secondary Battery. *Carbon* **2006**, *44*, 724−729.

(2) Pol, V. G.; Thackeray, M. M. Spherical Carbon Particles and Carbon Nanotubes Prepared by Autogenic Reactions: Evaluation as Anodes in Lithium Electrochemical Cells. *Energy Environ. Sci.* **2011**, *4*, 1904−1912.

(3) Vallet-Regí, M.; Balas, F.; Arcos, D. Mesoporous Materials for Drug Delivery. *Angew. Chem. Int. Ed* **2007**, *46*, 7548−7558.

(4) Champion, J. A.; Katare, Y. K.; Mitragotri, S. Particle Shape: A New Design Parameter for Micro- and Nanoscale Drug Delivery Carriers. *J. Controlled Release* **2007**, *121*, 3−9.

(5) Xu, X.; Friedman, G.; Humfeld, K. D.; Majetich, S. A.; Asher, S. A. Superparamagnetic Photonic Crystals. *Adv. Mater.* **2001**, *13*, 1681−1684.

(6) Sun, X.; Li, Y. Colloidal Carbon Spheres and Their Core/Shell Structures with Noble Metal Nanoparticles. *Angew. Chem. Int. Ed* **2004**, *43*, 597−601.

(7) Shipway, A. N.; Katz, E.; Willner, I. Nanoparticle Arrays on Surfaces for Electronic, Optical, and Sensor Applications. *ChemPhysChem* **2000**, *1*, 18−52.

(8) Peng, Q.; Dong, Y.; Li, Y. ZnSe Semiconductor Hollow Microspheres. *Angew. Chem. Int. Ed.* **2003**, *42*, 3027−3030.

(9) Jeong, U.; Wang, M.; Xia, X. Some New Developments in the Synthesis, Functionalization, and Utilization of Monodisperse Colloidal Spheres. *Adv. Funct. Mater.* **2005**, *15*, 1907−1921.

(10) Chai, G. S.; Yoon, S. B.; Kim, J. H.; Yu, J. S. Spherical Carbon Capsules with Hollow Macroporous Core and Mesoporous Shell Structures as a Highly Efficient Catalyst Support in the Direct Methanol Fuel Cell. *Chem. Commun.* **2004**, 2766−2767.

(11) Ge, J.; Huynh, T.; Hu, Y.; Yin, Y. Hierarchical Magnetite/Silica Nanoassemblies as Magnetically Recoverable Catalyst-supports. *Nano Lett.* **2008**, *8*, 931−934.

(12) Pekala, R. W. Organic Aerogels from the Polycondensation of Resorcinol with Formaldehyde. *J. Mater. Sci.* **1989**, *24*, 3221−3227.

(13) Lu, X.; Arduini-Schuster, M. C.; Kuhn, J.; Nilsson, O.; Fricke, J.; Pekala, R. W. Thermal Conductivity of Monolithic Organic Aerogels. *Science* **1992**, *225*, 971−972.

(14) ElKhatat, A. M.; Al-Muhtaseb, S. A. Advances in Tailoring Resorcinol−Formaldehyde Organic and Carbon Gels. *Adv. Mater.* **2011**, *23*, 2887−2903.

(15) Wu, D.; Fu, R.; Zhang, S.; Dresselhaus, M. S.; Dresselhaus, G. Preparation of Low-density Carbon Aerogels by Ambient Pressure Drying. *Carbon* **2004**, *42*, 2033−2039.

(16) Probstle, H.; Wiener, M.; Fricke, J. Carbon Aerogels for Electrochemical Double Layer Capacitors. *J. Porous Mater.* **2003**, *10*, 213−222.

(17) Stöber, W.; Fink, A.; Bohn, E. J. Controlled Growth of Monodisperse Silica Spheres in the Micron Size Range. *J. Colloid Interface Sci.* **1968**, *26*, 62−69.

(18) Scherdel, C.; Scherb, T.; Reichenauer, G. Spherical Porous Carbon Particles Derived from Suspensions and Sediments of Resorcinol−Formaldehyde Particles. *Carbon* **2009**, *47*, 2244−2252.

(19) Li, W. C.; Reichenauer, G. J. Fricke, Carbon Aerogels Derived from Cresol−Resorcinol−Formaldehyde for Supercapacitors. *Carbon* **2002**, *40*, 2955−2959.

(20) Pekala, R. W. Alviso, C. T.; Lemay, J. D. In *Chemical Processing of Advanced Materials*; Hench, L. L., West, J. K., Eds.; John Wiley and Sons: New York, 1992; p 671.

(21) Li, W.-C.; Lu, A.-H.; Schth, F. Preparation of Monolithic Carbon Aerogels and Investigation of Their Pore Interconnectivity by a Nanocasting Pathway. *Chem. Mater.* **2005**, *17*, 3620−3626.

(22) Dong, Y.-R.; Nishiyama, N.; Egashira, Y.; Ueyama, K. Basic Amid Acid-Assisted Synthesis of Resorcinol−Formaldehyde Polymer and Carbon Nanospheres. *Ind. Eng. Chem. Res.* **2008**, *47*, 4712−4716.

(23) Liu, J.; Zhang Qiao, S.; Liu, H.; Chen, J.; Orpe, A.; Zhao, D.; Lu, G. Q. Extension of The Stöber Method to the Preparation of Monodisperse Resorcinol−Formaldehyde Resin Polymer and Carbon Spheres. *Angew. Chem., Int. Ed.* **2011**, *50*, 5947−5951.

(24) Hao, G.-P.; Li, W.-C.; Qian, D.; Lu, A.-H. Rapid Synthesis of Nitrogen-Doped Porous Carbon Monolith for CO_2 Capture. *Adv. Mater.* **2010**, *22*, 853−857.

(25) Zhu, Y.; Hu, H.; Li, W.; Zhang, X. Resorcinol−Formaldehyde Based Porous Carbon as an Electrode Material for Supercapacitors. *Carbon* **2007**, *45*, 160−165.

(26) Horikawa, R.; Hayashi, J.; Muroyama, K. Size Control and Characterization of Spherical Carbon Aerogel Particles from Resorcinol−Formaldehyde Resin. *Carbon* **2004**, *42*, 169−175.

(27) Fuertes, A. B.; Valle-Vigón, P.; Sevilla, M. One-Step Synthesis of Silica@resorcinol−formaldehyde Spheres and Their Application for the Fabrication of Polymer and Carbon Capsules. *Chem. Commun.* **2012**, *48*, 6124−6126.

(28) Moreno, A. H.; Arenillas, A.; Calvo, E. G.; Bermúdez, J. M.; Menéndez, J. A. Carbonisation of Resorcinol−Formaldehyde Organic Xerogels: Effect of Temperature, Particle Size, and Heating Rate on the Porosity of Carbon Xerogels. *J. Anal. Appl. Pyrolysis* **2013**, *100*, 11−116.

(29) Gaca, K. Z.; Sefcik, J. Mechanism and Kinetics of Nanostructure Evolution during Early Stages of Resorcinol−Formaldehyde Polymerization. *J. Colloid Interface Sci.* **2013**, *406*, 51−59.

(30) Egorin, A. M.; Tutov, M. V.; Slobodyuk, A. B.; Avramenko, V. A. Stability of Resorcinol−Formaldehyde Resins in Alkaline Solutions. *Radiochemistry* **2014**, *56*, 183−188.

(31) Yu, J.; Guo, M.; Muhammad, F.; Wang, A.; Zhang, F.; Li, Q.; Zhu, G. One-pot Synthesis of Highly Ordered Nitrogen-containing Mesoporous Carbon with Resorcinol−Urea−Formaldehyde Resin for CO_2 Capture. *Carbon* **2014**, *69*, 502−514.

(32) Suslick, K. S.; Price, G. J. Applications of Ultrasound to Materials Chemistry. *Annu. Rev. Mater. Sci.* **1999**, *29*, 295−326.

(33) Didenko, Y. T.; McNamara, W. B., III; Suslick, K. S. Hot Spot Conditions during Cavitation in Water. *J. Am. Chem. Soc.* **1999**, *121*, 5817−5818.

(34) Gong, C.; Hart, D. P. Ultrasound Induced Cavitation and Sonochemical Yields. *J. Acoust. Soc. Am.* **1998**, *104*, 2675.

(35) *Ultrasound: Its Chemical, Physical, and Biological Effects*; Suslick, K. S., Ed.; VCH Publishers: New York, 1988.

(36) Tonanon, N.; Siyasukh, A.; Tanthapanichakoon, W.; Nishihara, H.; Mukai, S. R.; Tamon, H. Improvement of Mesoporosity of Carbon Cryogels by Ultrasonic Irradiation. *Carbon* **2005**, *43*, 525−531.

(37) Lu, A.-H.; Hao, G.-P.; Sun, Q. Can Carbon Spheres Be Created through the Stöber Method? *Angew. Chem., Int. Ed.* **2011**, *50*, 9023−9025.

(38) Brinker, C. J.; Scherer, G. W. *Sol-Gel Science: The Physics and Chemistry of Sol-Gel Processing*; Academic Press: New York, 1990.
(39) Giuntini, J. C.; Jullien, D.; Zanchetta, J. V.; Carmona, F.; Delhaes, P. Electrical Conductivity of Low-Temperature Carbons as a Function of Frequency. *J. Non-Cryst. Solids* **1978**, *30*, 87−98.
(40) Pol, V. G. Upcycling: Converting Waste Plastics into Paramagnetic, Conducting, Solid, Pure Carbon Microspheres. *Environ. Sci. Technol.* **2010**, *44*, 4753−4759.
(41) Jänes, A.; Kurig, H.; Lust, E. Characterisation of Activated Nanoporous Carbon for Supercapacitor Electrode Materials. *Carbon* **2007**, *45*, 1226−1233.
(42) 34Li, Z. Q.; Lu, C. J.; Xia, Z. P.; Zhou, Y.; Luo, Z. X-ray Diffraction Patterns of Graphite and Turbostratic Carbon. *Carbon* **2007**, *45*, 1686−1695.
(43) Elsayed, M. A.; Hall, P. J.; Heslop, M. J. Preparation and Structure Characterization of Carbons Prepared from Resorcinol−Formaldehyde Resin by CO_2 Activation. *Adsorption* **2007**, *13*, 299−306.
(44) Sharma, C. S.; Patil, S.; Saurabh, S.; Sharma, A.; Venkataraghavan, R. Resorcinol−Formaldehyde Based Carbon Nanospheres by Electrospraying. *Bull. Mater. Sci.* **2009**, *32*, 239−246.
(45) Wang, Y.; Su, F.; Wood, C. D.; Lee, J. Y.; Zhao, X. S. Preparation and Characterization of Carbon Nanospheres as Anode Materials in Lithium-Ion Secondary Batteries. *Ind. Eng. Chem. Res.* **2008**, *47* (7), 2294−2300.
(46) Zhang, J.; Wang, Y.; Zang, J.; Xin, G.; Yuan, Y.; Qu, X. Electrophoretic Deposition of MnO_2-Coated Carbon Nanotubes on a Graphite Sheet as a Flexible Electrode for Supercapacitors. *Carbon* **2012**, *50*, 5196−5202.
(47) Tao, Y.; Endo, M.; Ohsawa, R.; Kanoh, H.; Kaneko, K. High Capacitance Carbon-based Xerogel film Produced without Critical Drying. *Appl. Phys. Lett.* **2008**, *93*, 193112.
(48) Wilgosz, K.; Chen, X.; Kierzek, K.; Machnikowski, J.; Kalenczuk, R.; Mijowska, E. Template Method Synthesis of Mesoporous Carbon Spheres and Its Applications as Supercapacitors. *Nanoscale Res. Lett.* **2012**, *7*, 269.
(49) Chen, J.; Xia, N.; Zhou, T.; Tan, S.; Jiang, F.; Yuan, D. Mesoporous Carbon Spheres: Synthesis, Characterization, and Supercapacitance. *Int. J. Electrochem. Sci.* **2009**, *4*, 1063−1073.
(50) Kicinski, W.; Szala, M.; Bystrzejewski, M. Sulfur-Doped Porous Carbons: Synthesis and Applications. *Carbon* **2014**, *68*, 1−32.
(51) Bull. Kicinski, W.; Bystrzejewski, M.; Rummeli, M. H.; Gemming, T. Porous Graphitic Materials Obtained from Carbonization of Organic Xerogels Doped with Transition Metal Salts. *Bull. Mater. Sci.* **2014**, *37*, 141−150.